Astrophysical Journal Letters
Preprint typeset using LaTeX style emulateapj v. 6/22/04

A NEW MILKY WAY DWARF SATELLITE IN CANES VENATICI

D. B. Z [1], V. B [1], N. W. E [1], M. I. W [1], M. J. I [1], T. S [2], S. H [1], D. M. B [1], J. M. I [1], G. G [1], B. W [3], S. V [1], M. F [1], P. C. H [1], T. C. B [2], E. F. B [4], E. K. G [5], D. P. S [6], H. J. N [7], R. F. G. W [8], C. M. R [9], B. Y [10], R. L [11], J. A. S [12], J. C. B [13], H. B [13], J. B [13], M. H [13], S. J. K [13], J. K [13,14], D. L [13], A. N [13], S. A. S [13]

Astrophysical Journal Letters

ABSTRACT

In this Letter, we announce the discovery of a new dwarf satellite of the Milky Way, located in the constellation Canes Venatici. It was found as a stellar overdensity in the North Galactic Cap using Sloan Digital Sky Survey Data Release 5 (SDSS DR5). The satellite's color-magnitude diagram shows a well-defined red giant branch, as well as a horizontal branch. As judged from the tip of the red giant branch, it lies at a distance of ~ 220 kpc. Based on the SDSS data, we estimate an absolute magnitude of $M_V \sim -7.9$, a central surface brightness of $\mu_{0,V} \sim 28$ mag arcsecond^{-2}, and a half-light radius of $\sim 8\farcm5$ (~ 550 pc at the measured distance). The outer regions of Canes Venatici appear extended and distorted. The discovery of such a faint galaxy in proximity to the Milky Way strongly suggests that more such objects remain to be found.

Subject headings: galaxies: dwarf — galaxies: individual (Canes Venatici) — Local Group

1. INTRODUCTION

There are ten known dwarf spheroidal (dSph) companions of the Milky Way Galaxy. Together with the two dwarf irregulars (the Large and Small Magellanic Clouds), this makes up all the known satellite galaxies of the Milky Way. The dSphs have such low surface brightness that they have often been found serendipitously. For example, while Sextans (Irwin et al. 1990) was found as part of an automated search, the intrinsically far more luminous Sagittarius dSph was first identified kinematically from a radial velocity survey of stars in Galactic Center fields (Ibata et al. 1995).

As such galaxies are resolvable into individual stars because of their proximity, they are detectable as enhancements in the stellar number density in large photometric surveys. For example, Martin et al. (2004) analyzed overdensities of M giants in the 2MASS All Sky Survey and claimed the detection of a new disrupted dSph in Canis Major, although this remains controversial. Willman et al. (2005) systematically surveyed ~ 5800 square degrees of the Sloan Digital Sky Survey (SDSS; York et al. 2000) and identified a dSph companion to the Milky Way in the constellation of Ursa Major. Subsequent spectroscopic observations (Kleyna et al. 2005) showed that Ursa Major was a dark matter dominated dSph. Meanwhile, Zucker et al. (2004, 2006) announced the discovery of Andromeda IX and X, new dSph satellites of M31 found in SDSS data with similar methods.

Very recently, Belokurov et al. (2006b) mapped out the stars satisfying the color cut $g - r < 0.4$ in almost all of SDSS Data Release 5 (DR5). They dubbed this plot of the high-latitude Galactic northern hemisphere the "Field of Streams", owing to its wealth of prominent stellar substructure. Visible by eye in the plot is a heretofore undetected enhancement of the stellar density, located in the constellation Canes Venatici. Here, we show that this corresponds to a new dSph companion – the eleventh – of the Milky Way Galaxy.

TABLE 1
P C V D

Parameter[a]	
Coordinates (J2000)	13:28:03.5 +33:33:21.0±10″
Galactic Coordinates (*l*,*b*)	74.3, 79.8
Position Angle	73° ± 3°
Ellipticity	0.38
r_h (Plummer)	$8\farcm5 \pm 0\farcm5$
r_h (Exponential)	$8\farcm4 \pm 0\farcm5$
A_V	$0\fm05$
$\mu_{0,V}$ (Plummer)	$28\fm2 \pm 0\fm5$
$\mu_{0,V}$ (Exponential)	$27\fm8 \pm 0\fm5$
V_{tot}	$13\fm9 \pm 0\fm5$
$(m-M)_0$	$21\fm75 \pm 0\fm15$
$M_{tot,V}$	$-7\fm9 \pm 0\fm5$

[a]Surface brightnesses and integrated magnitudes are corrected for the mean Galactic foreground reddenings, A_V, shown.

2. DATA AND DISCOVERY

The SDSS is an imaging and spectroscopic survey. SDSS imaging data are produced in five photometric bands, namely *u*, *g*, *r*, *i*, and *z* (Fukugita et al. 1996; Gunn et al. 1998; Hogg et al. 2001; Adelman-McCarthy et al. 2006;

[1] Institute of Astronomy, University of Cambridge, Madingley Road, Cambridge CB3 0HA, UK; zucker,vasily,nwe@ast.cam.ac.uk
[2] Department of Physics and Astronomy, CSCE: Center for the Study of Cosmic Evolution, and JINA: Joint Institute for Nuclear Astrophysics, Michigan State University, East Lansing, MI 48824
[3] Center for Cosmology and Particle Physics, Department of Physics, New York University, 4 Washington Place, New York, NY 10003
[4] Max Planck Institute for Astronomy, Königstuhl 17, 69117 Heidelberg, Germany
[5] Astronomical Institute of the University of Basel, Department of Physics and Astronomy, Venusstrasse 7,CH-4102 Binningen, Switzerland
[6] Department of Astronomy and Astrophysics, Pennsylvania State University, 525 Davey Laboratory, University Park, PA 16802
[7] Rensselaer Polytechnic Institute, Troy, NY 12180
[8] The Johns Hopkins University, 3701 San Martin Drive, Baltimore, MD 21218
[9] Lick Observatory, University of California, Santa Cruz, CA 95064
[10] Fermi National Accelerator Laboratory, P.O. Box 500, Batavia, IL 60510
[11] Princeton University Observatory, Peyton Hall, Princeton, NJ 08544
[12] Los Alamos National Laboratory, ISR-4, MS D448, Los Alamos, NM 87545
[13] Apache Point Observatory, P.O. Box 59, Sunspot, NM 88349
[14] Mt. Suhora Observatory, Cracow Pedagogical University, ul. Podchorazych 2, 30-084 Cracow, Poland

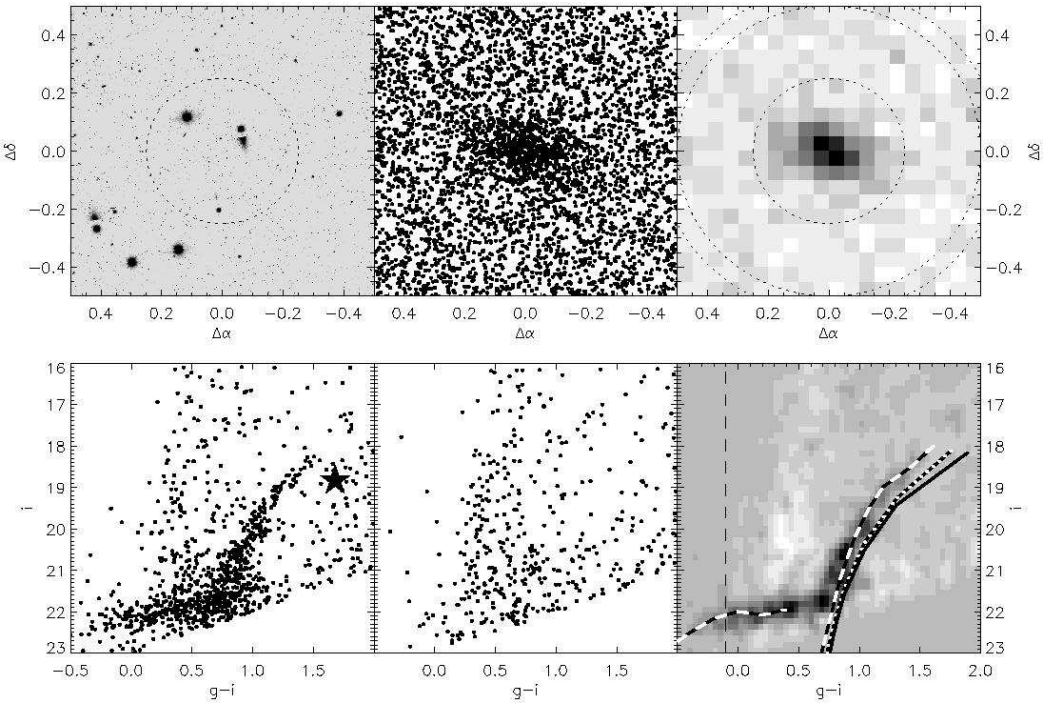

F . 1.— The Canes Venatici Dwarf: *Upper left:* Combined SDSS g, r, i images of a $1^\circ \times 1^\circ$ field centered on the overdensity. $\Delta\alpha$ and $\Delta\delta$ are the relative offsets in right ascension and declination, measured in arcdegrees. The dotted circle indicates a radius of 0.25°. *Upper middle:* The spatial distribution of all objects classified as stars in the same area. *Upper right:* Binned spatial density of all stellar objects. The inner dotted circle marks a radius of 0.25°, the middle circle a radius of 0.5°, and the outermost circle a radius of 0.56°. Bins are $0.05^\circ \times 0.05^\circ$, smoothed with a Gaussian with a FWHM of 0.1°. *Lower left:* CMD of all stellar objects within the inner 0.25° radius circle; note the clear RGB, with hints of a horizontal branch, even without removal of field contamination. The filled star shows the location of a carbon star in the field of CVn (see text). *Lower middle:* CMD of a comparably-sized control area, showing all stellar objects between 0.5° (middle circle) and 0.56° (outer circle) of the center. *Lower right:* A color-magnitude density plot (Hess diagram), showing the inner CMD minus a control CMD taken from between 0.5° and 2° of the center, normalized to the number of stars in each CMD. RGB and horizontal branch fiducial ridgelines derived from SDSS photometry of the globular cluster NGC 2419 ([Fe/H] ~ -2.1) are overplotted as dashed white-and-black lines; RGB fiducials for M 3 ([Fe/H] ~ -1.6) and M 71 (~ -0.7) from Clem (2005) are shown in dotted white-and-black and solid black, respectively. All fiducials were corrected for Galactic foreground extinction (Schlegel et al. 1998), and shifted to a distance modulus of 21.75. The thin dashed vertical line shows the cut $g - i < -0.1$ used to select candidate blue horizontal branch stars.

Gunn et al. 2006), and are automatically processed through pipelines to measure photometric and astrometric properties (Lupton, Gunn, & Szalay 1999; Stoughton et al. 2002; Smith et al. 2002; Pier et al. 2003; Ivezić et al. 2004). DR5 primarily covers $\sim$ 8000 square degrees around the North Galactic Pole (NGP).

In the process of analyzing this area of the NGP (Belokurov et al. 2006b), we visually identified a stellar overdensity in the constellation Canes Venatici. The upper left panel of Figure 1 shows a grayscale SDSS image of the sky centered on the stellar overdensity; note that no obvious object can be seen. However, a roughly elliptical overdensity of objects classified by the SDSS pipeline as stars is readily visible in the photometric data (upper middle and right panels). Plotting these stars in a color-magnitude diagram (CMD) reveals a clear red giant branch (RGB) and horizontal branch (lower panels). This CMD appears similar to that seen in SDSS data for the Sextans dSph (see, e.g., Fig. 1 of Willman et al. 2005), although considerably more distant. Based on its apparent morphology and on the presence of a distinct stellar population, we conclude that this is most likely a hitherto unknown dSph galaxy. As is customary, we name it after its constellation, Canes Venatici (CVn).

3. PHYSICAL PROPERTIES AND STELLAR POPULATION

The distance of a distinct, metal-poor stellar population can be estimated from the I-band magnitude of the tip of the red giant branch (TRGB; e.g., Mould et al. 1983; Lee, Freedman, & Madore 1993). We applied the transforms from Smith et al. (2002) to convert dereddened SDSS g, r, i magnitudes to V, I magnitudes. The cumulative I-band luminosity function for the RGB shows a sharp rise starting at $I \sim 17.75$ (which corresponds to $i \sim 18.23$). The horizontal branch fit in the lower right panel of Figure 1 provides supporting evidence for the reliability of our procedure. Assuming a metallicity of [Fe/H]~ -2 (see below) and a TRGB color of $(V - I)_{\rm TRGB} = 1.4$, from the calibration of Da Costa & Armandroff (1990) we obtain the relation $(m - M)_0 = I_{\rm TRGB} + 3.97$, yielding a distance modulus of $(m - M)_0 \sim 21.75 \pm 0.20$ ($\sim 220^{+25}_{-16}$ kpc). This is comparable to the most distant Milky Way dSph satellites previously known, Leo I and II (250 and 215 kpc, respectively: Lee et al. 1993; Lee 1995).

The age and metallicity of the stars in CVn can be estimated by comparison with the CMDs of single epoch, single metallicity populations, e.g., Galactic globular clusters. In the lower right panel of Figure 1, we show a field-star-subtracted Hess diagrams (color-magnitude density plots) in $(i, g - i)$. Fiducial ridgelines of three globular clusters – NGC 2419 ([Fe/H] ~ -2.1), M 3 ([Fe/H] ~ -1.6), and M 71 ([Fe/H] ~ -0.7) – are overplotted from left to right. The best match is to NGC 2419, and in combination with the prominent horizontal branch, the similarity indicates that CVn is dominated by an old, metal-poor ([Fe/H] ~ -2) stellar population. The horizontal branch extends very far to the blue, although it is predominantly red. Such red-dominated horizontal branches,

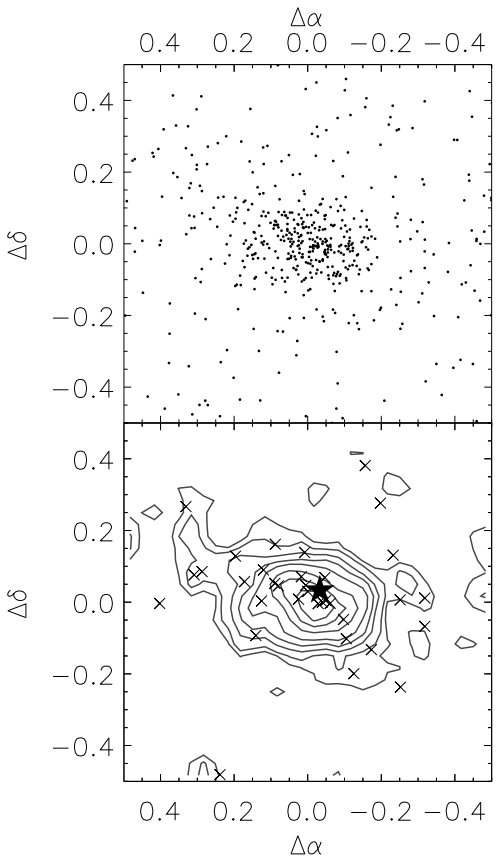

F . 2.— Morphology of the CVn dwarf: *Upper:* The spatial distribution of stars selected from CMD regions with the highest contrast between CVn and field stellar populations. $\Delta\alpha$ and $\Delta\delta$ are relative offsets (arcdegrees) in right ascension and declination. *Lower:* A contour plot of the spatial distribution of these stars; candidate blue horizontal branch stars (from the area blueward of the dashed line in the lower right panel of Fig 1) are overplotted with crosses. The contours are 2, 3, 5, 7, 10, 15, 20, and 25σ above the background level. The location of the carbon star, SDSS J132755.56+333521.7, is indicated by the black star.

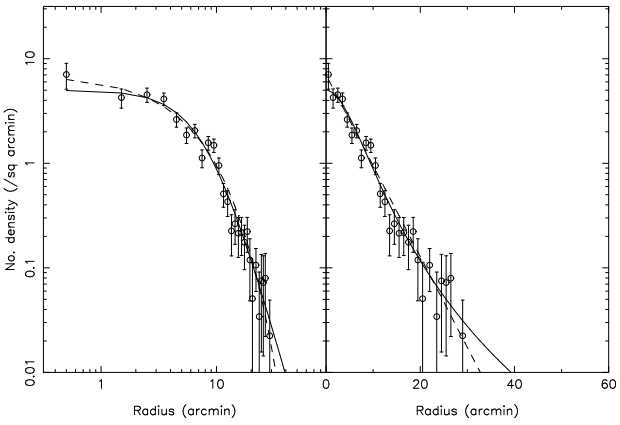

F . 3.— Profile of CVn, showing the background-subtracted stellar density in elliptical annuli as a function of mean radius. The left panel is logarithmic in both axes, and the right panel is linear in radius. The overplotted lines are fitted Plummer (solid) and exponential (dashed) profiles.

hinting at a range of ages in the stellar population, are also seen in other metal-poor dSphs (e.g., Harbeck et al. 2001).

To investigate the spatial morphology, we select candidate members by applying a mask built as follows. First, we find the class conditional probabilities $P_{\rm CVn}$ and $P_{\rm bg}$ (see e.g., Belokurov et al. 2006a) of a star belonging to CVn and the

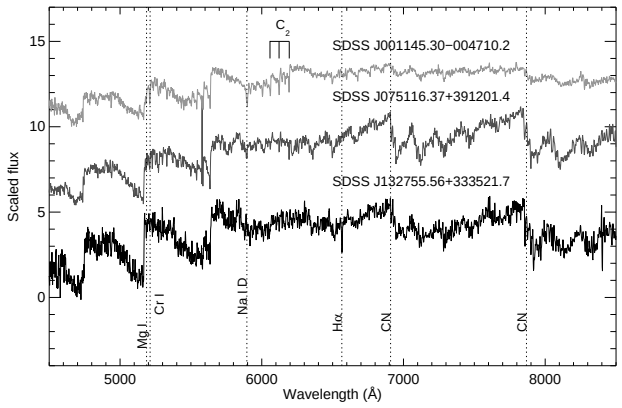

F . 4.— Spectrum of SDSSJ132755.56+333521.7 (*bottom*), a carbon star located near the center of CVn (see lower left panel of Figure 1 and the lower panel of Figure 2). Spectra of a giant carbon star (SDSSJ075116.37+391201.4, *middle*) and a dwarf carbon star (SDSSJ001145.30-004710.2, *top*) with similar temperatures ($T_{\rm eff}$ ~ 4000K; Downes et al. 2004) are shown for comparison. The CN bands are stronger in the reference giant than in the dwarf, while Na I, Cr I, and Mg Ib lines and the C_2 bands around 6150 Å are stronger in the dwarf. The strength of the former and weakness of the latter features in SDSSJ132755.56+333521.7 indicate that it is most likely a giant carbon star in CVn.

background, respectively. These are just the normalized Hess diagrams. The ratio of the class conditional probabilities $x = P_{\rm CVn}/P_{\rm bg}$ is converted to a probability of membership of CVn via $p = x/(1+x)$. A cut of $p > 0.8$ is used to select stars plotted in the top panel of Fig. 2. These objects are binned into 30×30 bins, each $0.033^\circ \times 0.033^\circ$, and smoothed with a Gaussian with FWHM of 0.067° to yield the plot in the lower panel. The density contours, representing 2, 3, 5, 7, 10, 15, 20, and 25σ above the background level, are markedly irregular, particularly in the outer parts – somewhat reminiscent of the Ursa Minor dSph. The black crosses are candidate blue horizontal branch stars (BHBs) selected with $g-i < -0.1$. The distribution of BHBs is elongated in the same manner as the density contours and traces the same underlying morphology.

To estimate the properties listed in Table 1, we first analyze the morphology shown in Figure 2 to derive the centroid from the density-weighted first moment of the distribution, and the average ellipticity and position angle using the three density-weighted second moments (e.g., Stobie 1980). The radial profile shown in Figure 3 is derived by computing the average density within elliptical annuli after first subtracting a constant asymptotic background level (0.25 arcminute^{-2}) reached at large radii. We then fit the radial profile with standard Plummer and exponential laws (Figure 3, see also Irwin & Hatzidimitriou 1995). The best-fitting position angle, ellipticity and half-light radii are listed in Table 1. At the distance of CVn, the approximately 8.′5 half-light radius corresponds to ~ 550 pc. The overall extent is ~ 2 kpc along the major axis, making CVn one of the largest of the Milky Way dSphs. Although Plummer and exponential laws provide reasonable fits to the data, there are some discrepant datapoints in Figure 3 (cf. Sextans' profile in Irwin & Hatzidimitriou 1995).

The overall luminosity is computed by masking the stellar locus of CVn and computing the total flux within the mask and within the elliptical half-light radius. A similar mask, but covering a larger area to minimize shot-noise, well outside the main body of CVn, is scaled by relative area and used to compute the foreground contamination within the half-light radius. After correcting for this contamination, the remaining

flux is scaled to the total, assuming the fitted profiles are a fair representation of the overall flux distribution. We also apply a correction of 0.5 magnitudes for unresolved/faint stars, based on the stellar luminosity functions of other low metallicity, low surface brightness dSphs. The resulting luminosity and central surface brightness estimates, $M_{tot,V} \sim -7.9$ and $\mu_{0,V} \sim 28$ mag arcsec^2, are roughly consistent with the central surface brightness – absolute magnitude relation noted for Local Group dSph satellites (e.g., Grebel, Gallagher, & Harbeck 2003). However, CVn lies far from the central surface brightness – host galaxy distance correlation found for other Local Group dSph satellites (e.g., Fig. 7 of McConnachie & Irwin 2006), suggesting that this correlation may be at least partially due to observational biases (e.g., Willman et al. 2004).

A search of the SDSS DR5 spectroscopic database revealed the spectrum of a CH carbon star, SDSS J132755.56+333521.7, in close proximity to the center of CVn (lower panel of Figure 2). As shown in Figure 4, the star's spectral features indicate that it is most likely a giant, rather than a dwarf. There are no 2MASS point sources within 15″, and a comparison of the SDSS coordinates with earlier-epoch APM data is consistent with zero proper motion, both of which would argue in favor of its being a distant object. Finally, the carbon star's dereddened *r*-band magnitude is 19.18; at the calculated distance modulus for CVn, ∼ 21.75, the star would have an absolute magnitude $M_r \sim -2.5$, fairly typical of a CH carbon giant. Hence we conclude that SDSS J132755.56+333521.7 is a carbon star in CVn. We measure a heliocentric radial velocity of $+36 \pm 20$ km s^{-1} for the carbon star from cross-correlation with the spectrum of another CH carbon star of known velocity (1249+0146, see Totten & Irwin 1998). The carbon star's radial velocity in the line of sight direction (after correction to the Galactic rest frame) is $\sim 80 \pm 20$ km s^{-1}. Given the distance of CVn, this is also approximately the radial velocity that would be seen from the Galactic Center. We plan to obtain follow-up spectroscopy of RGB stars in CVn to supplement this first estimate of its systemic velocity with a more detailed analysis of the new dwarf's kinematics.

4. CONCLUSIONS

We have discovered a new dwarf spheroidal Milky Way satellite in the constellation Canes Venatici. It has an absolute magnitude of $M_V \sim -7.9$ and a surface brightness of $\mu_{0,V} \sim 28$ mag arcsecond^{-2}. We find that CVn is dominated by an old, metal-poor ([Fe/H] ∼ −2) stellar population. At a distance of ∼ 220 kpc, CVn is one of the most remote of the known dSph companions to the Milky Way.

It is important to carry out a well-defined census of Milky Way dwarf galaxies to the faintest possible luminosities. Numerical simulations in Cold Dark Matter cosmological models predict that the Milky Way's halo should contain about 500 satellites comparable to the dSphs (Moore et al. 1999; Klypin et al. 1999). This contrasts with the handful of known Milky Way dSphs. The new dSph in Canes Venatici, taken with the recent discovery of Ursa Major (Willman et al. 2005), emphasizes how incomplete our current knowledge is. Further analysis of photometric data from large-area digital surveys such as SDSS will thus likely lead to the discovery of more dSphs around the Milky Way in the near future.

DBZ, VB, MIW, DMB and MF acknowledge the financial support of the Particle Physics and Astronomy Research Council of the United Kingdom.

Funding for the SDSS and SDSS-II has been provided by the Alfred P. Sloan Foundation, the Participating Institutions, the National Science Foundation, the U.S. Department of Energy, the National Aeronautics and Space Administration, the Japanese Monbukagakusho, the Max Planck Society, and the Higher Education Funding Council for England. The SDSS Web Site is http://www.sdss.org/.

The SDSS is managed by the Astrophysical Research Consortium for the Participating Institutions. The Participating Institutions are the American Museum of Natural History, Astrophysical Institute Potsdam, University of Basel, Cambridge University, Case Western Reserve University, University of Chicago, Drexel University, Fermilab, the Institute for Advanced Study, the Japan Participation Group, Johns Hopkins University, the Joint Institute for Nuclear Astrophysics, the Kavli Institute for Particle Astrophysics and Cosmology, the Korean Scientist Group, the Chinese Academy of Sciences (LAMOST), Los Alamos National Laboratory, the Max-Planck-Institute for Astronomy (MPIA), the Max-Planck-Institute for Astrophysics (MPA), New Mexico State University, Ohio State University, University of Pittsburgh, University of Portsmouth, Princeton University, the United States Naval Observatory, and the University of Washington.

REFERENCES

Adelman-McCarthy, J. K., et al. 2006, ApJS, 162, 38
Belokurov, V., Evans, N. W., Irwin, M. J., Hewett, P. C., & Wilkinson, M. I. 2006a, ApJ, 637, L29
Belokurov, V. et al. 2006, ApJ, in press
Clem, J. L. 2005, PhD Thesis, University of Victoria
Da Costa, G. S., & Armandroff, T. E. 1990, AJ, 100, 162
Downes, R. A., et al. 2004, AJ, 127, 2838
Fukugita, M., Ichikawa, T., Gunn, J. E., Doi, M., Shimasaku, K., & Schneider, D. P. 1996, AJ, 111, 1748
Grebel, E. K., Gallagher, J. S., & Harbeck, D. 2003, AJ, 125, 1926
Gunn, J. E. et al. 1998, AJ, 116, 3040
Gunn, J. E. et al. 2006, ApJ, in press
Harbeck, D. et al. 2001, AJ, 122, 3092
Hogg, D.W., Finkbeiner, D.P., Schlegel, D.J., Gunn, J.E. 2001, AJ, 122, 2129
Ibata, R. A., Gilmore, G., & Irwin, M. J. 1995, MNRAS, 277, 781
Irwin, M., & Hatzidimitriou, D. 1995, MNRAS, 277, 1354
Irwin, M. J., Bunclark, P. S., Bridgeland, M. T., & McMahon, R. G. 1990, MNRAS, 244, 16P
Ivezić, Ž. et al., AN, 325, 583
Kleyna, J. T., Wilkinson, M. I., Evans, N. W., & Gilmore, G. 2005, ApJ, 630, L141
Klypin, A., Kravtsov, A. V., Valenzuela, O., & Prada, F. 1999, ApJ, 522, 82
Lee, M. G., Freedman, W. L., & Madore, B. F. 1993, ApJ, 417, 553
Lee, M., Freedman, W., Mateo, M., Thompson, I., Roth, M., and Ruiz, M. 1993, AJ, 106, 1420
Lee, M. 1995, AJ, 110, 1155
Lupton, R., Gunn, J., & Szalay, A. 1999, AJ, 118, 1406
Martin, N. F., Ibata, R. A., Bellazzini, M., Irwin, M. J., Lewis, G. F., & Dehnen, W. 2004, MNRAS, 348, 12
McConnachie, A., & Irwin, M. 2006, MNRAS, 365, 1263
Moore, B., Governato, F., Lake, G., Quinn, T., Stadel, J., & Tozzi, P. 1999, ApJ, 524, L19
Mould, J., Kristian, J., & Da Costa, G. 1983, ApJ, 270, 471
Pier, J.R., Munn, J.A., Hindsley, R.B, Hennessy, G.S., Kent, S.M., Lupton, R.H., Ivezic, Z. 2003, AJ, 125, 1559
Schlegel, D. J., Finkbeiner, D. P., & Davis, M. 1998, ApJ, 500, 525
Smith, J. A., et al. 2002, AJ, 123, 2121
Stobie, R.S., 1980, JBIS, 33, 323.
Stoughton, C. et al. 2002, AJ, 123, 485
Totten, E. J., & Irwin, M. J. 1998, MNRAS, 294, 1
Willman, B., Governato, F., Dalcanton, J. J., Reed, D., & Quinn, T. 2004, MNRAS, 353, 639
Willman, B., et al. 2005, ApJ, 626, L85
York D.G., et al. 2000, AJ, 120, 1579
Zucker, D. B., et al. 2004, ApJ, 612, L121
Zucker, D. B., et al. 2006, ApJ, submitted (astro-ph/0601599)